Journal of Systems Engineering and Electronics
Vol. PP, No. 99, June 2024, pp.1 – 11

Channel estimation in integrated radar and communication systems with power amplifier distortion

LIU Yan[1], YI Jianxin[1,*], WAN Xianrong[1], RAO Yunhua[1,2], and HAO Caiyong[1,3]

1. School of Electronic Information, Wuhan University, Wuhan 430072, China; 2. Shenzhen Research Institute of Wuhan University, Shenzhen 518057, China; 3. State Radio Monitoring Center of China, Shenzhen 518120, China

Abstract: To reduce the negative impact of the power amplifier (PA) nonlinear distortion caused by the orthogonal frequency division multiplexing (OFDM) waveform with high peak-to-average power ratio (PAPR) in integrated radar and communication (RadCom) systems is studied, the channel estimation in passive sensing scenarios. Adaptive channel estimation methods are proposed based on different pilot patterns, considering nonlinear distortion and channel sparsity. The proposed methods achieve sparse channel results by manipulating the least squares (LS) frequency-domain channel estimation results to preserve the most significant taps. The decision-aided method is used to optimize the sparse channel results to reduce the effect of nonlinear distortion. Numerical results show that the channel estimation performance of the proposed methods is better than that of the conventional methods under different pilot patterns. In addition, the bit error rate performance in communication and passive radar detection performance show that the proposed methods have good comprehensive performance.

Keywords: channel estimation, integrated radar and communication (RadCom), passive sensing, nonlinear distortion, power amplifier (PA), pilot pattern.

DOI: 10.23919/JSEE.2024.000053

1. Introduction

In recent years, to alleviate the spectrum resource shortage, spectrum sharing between radar and communication has attracted significant attention from industry and academia [1,2]. The integrated radar and communication (RadCom) technology has great significance in civil fields such as vehicle networking, low altitude monitoring, and smart home [3].

Downlink signal sensing is further classified as active sensing and passive sensing modes, and this paper focuses on passive sensing as an application scenario [4,5]. In the active sensing scenario, the radar has fully known the downlink signal. In the passive sensing scenario, the radar only obtains limited information such as the pilot data through the communication standard of the transmitter. Passive radar, a pioneering technology of the joint of radar and communication, realizes target detection and tracking by utilizing existing opportunistic illuminators. It has the advantages of spectrum saving and security, however, its performance is affected by the illuminator [6]. And common opportunistic illuminators use orthogonal frequency division multiplexing (OFDM) technology [7].

The OFDM technology has the advantages of high spectral efficiency and strong anti-multipath fading ability. However, the waveform's dynamic range is large, and the high peak-to-average power ratio (PAPR) leads to the power amplifier (PA) working in the nonlinear region [8]. In fact, high PAPR results in signal distortion that affects channel estimation in passive radar reference signal reconstruction as well as communication channel estimation and signal detection. However, reducing distortion with power fallback reduces PA efficiency and affects the operating range of the radiation source.

The nonlinear PA distortion based on receiver processing mainly focuses on three aspects. The first aspect is the theoretical analysis of communication systems affected by the nonlinear PA distortion. Banelli et al. [9] specifically analysed the influence of nonlinear distortion on the bit error rate (BER) of communication systems, and gave the theoretical BER expression in the additive white Gaussian noise (AWGN) channel. Zheng et al. [10] pointed out that the PA distorts the pilot and data in the digital video broadcasting for handheld (DVB-H) system, and analysed the overall impact of the system. The second aspect is the research on data distortion compensation assuming that the nonlinear PA distortion does not affect channel estimation. The optimum and sub-opti-

Manuscript received August 06, 2023.
*Corresponding author.
This work was supported by the National Natural Science Foundation of China (61931015;62071335;62250024), the Natural Science Foundation of Hubei Province of China (2021CFA002), the Fundamental Research Funds for the Central Universities of China (2042022dx0001), and the Science and Technology Program of Shenzhen (JCYJ20170818112037398).

mum detector for OFDM signals with strong nonlinear distortion was proposed in [11]. The third aspect is the study on the distortion compensation considering the degradation of channel estimation performance caused by the nonlinear distortion. Wu et al. and Ma et al. [12,13] proposed the decision-aided channel estimation method under nonlinear distortion. Joint channel estimation and detection schemes suitable for block pilot distribution were studied [14]. To mitigate the effect of the nonlinear distortion, some literature adopts data training based on deep learning to achieve channel estimation and signal detection [15−17].

The influence of nonlinear PA distortion on communication performance has attracted much attention in the past, but the fact that the quality of reference signal reconstruction in passive radar systems depends on channel estimation accuracy has been ignored [18]. Although existing channel estimation methods provide guidance for researchers, they ignore the two factors of nonlinear distortion and sparse time-domain channel. In the case of strong nonlinear distortion, direct use of the traditional least squares (LS) frequency-domain channel estimation can result in poor channel estimation performance [12]. In [11,13], the proposed channel estimation methods pay attention to nonlinear distortion but ignore the sparsity of time-domain channels. In addition, the design of random pilots to reduce the cost of pilots and alleviate the pollution of pilots has attracted much attention. In this case, the traditional LS channel estimation method is no longer applicable [19]. Channel estimation using compressed sensing theory can achieve good results. However, it is difficult to determine the channel sparsity or the iteration-stopping condition of the compressed sensing algorithm. Usually, the iteration stop threshold is empirical [20], or it is assumed that the receiver knows some prior information that is difficult to obtain in practice [21,22]. The channel estimation method [21] assumes a known signal to noise ratio (SNR). Similarly, the prior information is channel sparsity, which may change due to non-integer normalized path delay [22].

To solve the problem of channel estimation performance degradation caused by strong nonlinear PA distortion in the RadCom system for passive sensing, different adaptive channel estimation methods are proposed according to different pilot patterns. The proposed methods take both the PA distortion and sparse channels into account. Specifically, inspired by [12,13], we adopt the decision-aided method to reduce strong distortion according to the PA model. The determination of channel sparsity in the time domain is based on the result of LS channel estimation, and the main contributions are as follows:

(i) When the pilot pattern is uniform, it is difficult to determine the threshold for the most significant taps (MST) in the time domain. Based on the estimation of the maximum delay in the LS results, we get an effective threshold value through the nonlinear distortion compensation. Simulation results show that the proposed adaptive threshold channel estimation method is better than the existing methods.

(ii) For the random pilot pattern, the adaptive sparsity is got by comparing the channel noise with the valid threshold and then completing the channel estimation with decision-aided operation. Compared with the existing compressed sensing estimation methods with iterative stopping thresholds based on empirical values, the proposed adaptive sparsity method has a better overall performance.

This paper is organized as follows. Section 2 describes the system model considered, the PA model, and the traditional LS frequency-domain method involved in this paper. In Section 3, adaptive channel estimation methods considering both the PA distortion and sparse channels are proposed according to different pilot patterns. The results of channel estimates and corresponding communication and passive radar detection performance are shown in Section 4. Finally, Section 5 concludes this paper with potential future work.

2. System models

The RadCom system model for passive sensing scenarios is shown in Fig. 1. We consider a multicarrier system based on OFDM signal structure, and the PA causes the nonlinear signal distortion. The communication receiver restores the transmitted data based on the received signal, and the passive radar detects the target using the distorted signal, and the passive radar uses constant false alarm rate (CFAR) detectors to detect the target based on the distorted signal.

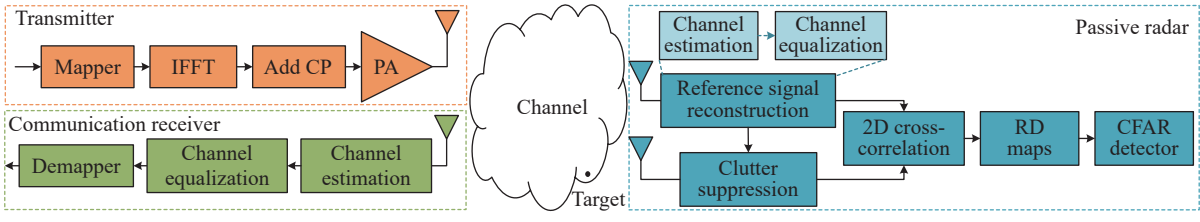

Fig. 1 RadCom system for passive sensing scenarios

2.1 Signal model

Assume that the OFDM system consists of N subcarriers, in which $\boldsymbol{X}=[X(0),X(1),\cdots,X(N-1)]^{\mathrm{T}}$ is the frequency-domain modulation symbol selected from the multiple quadrature amplitude modulation (MQAM) constellation. The time-domain signal is given as

$$x(t)=\frac{1}{\sqrt{N}}\sum_{k=0}^{N-1}X(k)\mathrm{e}^{\mathrm{j}2\pi\frac{k}{T_{\mathrm{u}}}(t-T_{\mathrm{g}})},\ 0\leqslant t<T_{\mathrm{u}} \tag{1}$$

where T_{g} and T_{u} are the guard interval duration and the useful part symbol duration, respectively. The corresponding discrete form is as follows:

$$x(n)=\frac{1}{\sqrt{N}}\sum_{k=0}^{N-1}X(k)\mathrm{e}^{\mathrm{j}2\pi\frac{kn}{N}},\ 0\leqslant n<N. \tag{2}$$

The cyclic prefix (CP) is added to the OFDM signal as the protection interval to eliminate the interference caused by multipath propagation. The baseband signal is amplified by the radio frequency (RF) PA and transmitted through the antenna. The structure of the CP-OFDM waveform is shown in Fig. 2. The maximum multipath delay τ usually meets $\tau\leqslant T_{\mathrm{g}}$.

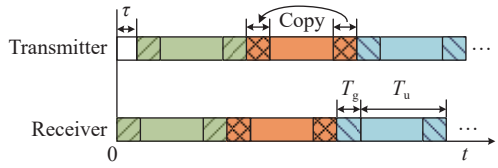

Fig. 2 Structure of the CP-OFDM waveform

The most common memoryless PAs are soft envelope limiters (SEL), traveling wave tube amplifiers (TWTA), and solid-state PA (SSPA). The previously widely used TWTA has been gradually replaced by the SSPA [23]. The SSPA model approaches the SEL property when the smoothness parameter in SSPA approaches infinity. This paper assumes that the signal generated by the modulator passes through the SEL, which is a simplified but useful model of the PA. Thus, the output signal of the PA [24] is

$$g[x(n)]=\begin{cases}x(n), & |x(n)|\leqslant A_{\mathrm{sat}}\\ A_{\mathrm{sat}}\mathrm{e}^{\mathrm{j}\theta(n)}, & |x(n)|>A_{\mathrm{sat}}\end{cases} \tag{3}$$

where A_{sat} is the PA input saturation amplitude, and $\theta(n)$ is the phase of $x(n)$. Although most physical devices do not exhibit this piecewise linear behavior exactly, the SEL is a good model after linearizing the nonlinear elements with suitable pre-distortion [25].

Then, the kth subcarrier output in the frequency-domain can be written as

$$Y(k)=[X(k)+C(k)]H(k)+w(k),\ 0\leqslant k<N \tag{4}$$

where $\boldsymbol{Y}=[Y(0),Y(1),\cdots,Y(N-1)]^{\mathrm{T}}\in\mathbf{C}^{N\times1}$ is the frequency-domain signal vector from the receiver. Similarly, $\boldsymbol{C}\in\mathbf{C}^{N\times1}$ is the nonlinear distortion vector caused by the PA, $\boldsymbol{H}\in\mathbf{C}^{N\times1}$ is the frequency-domain channel impulse response (CIR) vector, and $\boldsymbol{w}\in\mathbf{C}^{N\times1}$ is the AWGN vector.

Consider that P pilots are used to estimate sparse channels with an index set $I_{\mathrm{P}}=\{k_0,k_1,\cdots,k_{P-1}\}$. The received pilot vector $\boldsymbol{Y}_{\mathrm{P}}=[Y(k_0),Y(k_1),\cdots,Y(k_{P-1})]^{\mathrm{T}}\in\mathbf{C}^{P\times1}$ from the communication receiver or the passive radar reference channel is

$$\boldsymbol{Y}_{\mathrm{P}}=(\boldsymbol{X}_{\mathrm{P}}+\boldsymbol{C}_{\mathrm{P}})\boldsymbol{H}_{\mathrm{P}}+\boldsymbol{w}_{\mathrm{P}}=\boldsymbol{D}_{\mathrm{P}}\boldsymbol{H}_{\mathrm{P}}+\boldsymbol{w}_{\mathrm{P}} \tag{5}$$

where $\boldsymbol{X}_{\mathrm{P}}=\mathrm{diag}[X(k_0),X(k_1),\cdots,X(k_{P-1})]$ is the diagonal matrix of standard pilots, $\boldsymbol{C}_{\mathrm{P}}=\mathrm{diag}[C(k_0),C(k_1),\cdots,C(k_{P-1})]$ is the nonlinear distortion vector in the pilots, and $\boldsymbol{D}_{\mathrm{P}}\in\mathbf{C}^{P\times P}$ is the diagonal matrix of transmitted distorted pilots. $\boldsymbol{H}_{\mathrm{P}}\in\mathbf{C}^{P\times1}$ is the CIR in pilots, and $\boldsymbol{w}_{\mathrm{P}}\in\mathbf{C}^{P\times1}$ is the AWGN in the pilots. The complete frequency-domain CIR $\boldsymbol{H}\in\mathbf{C}^{N\times1}$ is obtained by interpolating based on $\boldsymbol{H}_{\mathrm{P}}$.

2.2 Traditional channel estimation method

Traditional channel estimate without considering pilot distortion is derived from the LS frequency-domain method

$$\hat{\boldsymbol{H}}_{\mathrm{P}}=\left(\boldsymbol{X}_{\mathrm{P}}{}^{\mathrm{H}}\boldsymbol{X}_{\mathrm{P}}\right)^{-1}\boldsymbol{X}_{\mathrm{P}}{}^{\mathrm{H}}\boldsymbol{Y}_{\mathrm{P}}=\boldsymbol{X}_{\mathrm{P}}{}^{-1}\boldsymbol{Y}_{\mathrm{P}}. \tag{6}$$

For clarity, the CIR at the kth subcarrier belonging to the pilots can be presented as

$$\hat{H}_{\mathrm{P}}(k)=\frac{Y_{\mathrm{P}}(k)}{X_{\mathrm{P}}(k)},\ k\in I_{\mathrm{P}}, \tag{7}$$

the complete CIR $\hat{\boldsymbol{H}}_{\mathrm{LS}}\in\mathbf{C}^{N\times1}$ is then obtained by interpolation.

Note that the frequency-domain CIR with the nonlinear PA distortion is derived as

$$\hat{H}'_{\mathrm{P}}(k)=\frac{Y_{\mathrm{P}}(k)}{X_{\mathrm{P}}(k)+C_{\mathrm{P}}(k)}=\frac{Y_{\mathrm{P}}(k)}{D_{\mathrm{P}}(k)},\ k\in I_{\mathrm{P}}. \tag{8}$$

3. Proposed channel estimation methods

From (6), traditional LS frequency-domain channel estimation ignores the effects of strong nonlinear distortion and channel sparsity. In this section, inspired by the decision-aided mitigation of strong nonlinear distortion [11,13] and preservation of the MST [20−22], we pro-

pose corresponding channel estimation methods based on different pilot patterns.

Assume that the maximum path delay is less than or equal to the CP time L_{cp}, and the received pilot in (5) can be rewritten as

$$\boldsymbol{Y}_{\mathrm{P}}=\boldsymbol{D}_{\mathrm{P}}\boldsymbol{F}_{P\times L_{\mathrm{cp}}}\boldsymbol{h}+\boldsymbol{w}_{\mathrm{P}}=\boldsymbol{A}\boldsymbol{h}+\boldsymbol{w}_{\mathrm{P}} \tag{9}$$

where $\boldsymbol{h}=[h(0),h(1),\cdots,h(L_{\mathrm{cp}}-1)]^{\mathrm{T}}$ is the time-domain sparse channel vector, $\boldsymbol{F}_{P\times L_{\mathrm{cp}}}$ is a discrete Fourier transform (DFT) submatrix, and $\boldsymbol{A}$ is the $P\times L_{\mathrm{cp}}$ measurement matrix. Specifically, $\boldsymbol{F}_{P\times L_{\mathrm{cp}}}$ is obtained by selecting the rows of the DFT matrix with the index set $I_{\mathrm{P}}=\{k_0,k_1,\cdots,k_{P-1}\}$ and the first L_{cp} columns. $\boldsymbol{F}_{P\times L_{\mathrm{cp}}}$ is presented as

$$\boldsymbol{F}_{P\times L_{\mathrm{cp}}}=\begin{bmatrix} W_N^{k_0 0} & W_N^{k_0 1} & \cdots & W_N^{k_0(L_{\mathrm{cp}}-1)} \\ W_N^{k_1 0} & W_N^{k_1 1} & \cdots & W_N^{k_1(L_{\mathrm{cp}}-1)} \\ \vdots & \vdots & & \vdots \\ W_N^{k_{P-1}0} & W_N^{k_{P-1}1} & \cdots & W_N^{k_{P-1}(L_{\mathrm{cp}}-1)} \end{bmatrix} \tag{10}$$

where $W_N^{kq}=\mathrm{e}^{-\mathrm{j}2\pi kq/N}$, $k\in I_{\mathrm{P}}$, $0\leqslant q<L_{\mathrm{cp}}$.

3.1 Uniform pilot pattern

Fig. 3 shows the uniform pilot pattern.

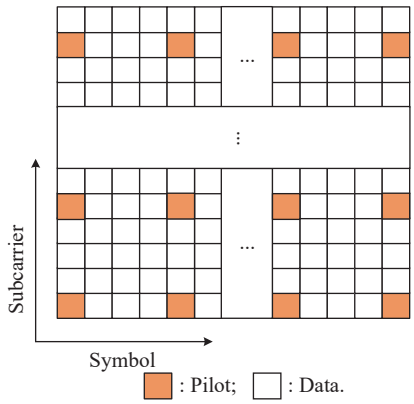

Fig. 3 Uniform pilot pattern

To get the true channel state information, existing radiation sources usually insert enough pilots to obtain more accurate results. Thus, $L_{\mathrm{cp}}\leqslant P<N$ can be assumed without loss of generality, the LS solution of the time-domain CIR in (9) is

$$\boldsymbol{h}_{\mathrm{LS}}=\left(\boldsymbol{A}^{\mathrm{H}}\boldsymbol{A}\right)^{-1}\boldsymbol{A}^{\mathrm{H}}\boldsymbol{Y}_{\mathrm{P}}=\boldsymbol{h}+\boldsymbol{h}_{\mathrm{n}} \tag{11}$$

where $\boldsymbol{h}_{\mathrm{n}}$ is the channel estimation noise vector.

$\boldsymbol{D}_{\mathrm{P}}$ and $\boldsymbol{h}_{\mathrm{n}}$ are the two main factors that affect the channel estimation results under strong nonlinear PA distortion. The channel estimation method proposed is as follows:

(i) Get the sparse channel in the time domain by adaptive threshold.

The initial value of the effective channel threshold T_{h} [26] is calculated as

$$T_{\mathrm{h}}=\sqrt{2\ln L_{\mathrm{cp}}}\sigma_{\mathrm{n}} \tag{12}$$

where σ_{n} is the standard deviation of the channel estimation noise vector $\boldsymbol{h}_{\mathrm{n}}$. Let $\boldsymbol{D}_{\mathrm{P}}=\boldsymbol{X}_{\mathrm{P}}$. The value of $\sigma_{\mathrm{n}}{}^2$ depends on the LS frequency-domain channel estimation results of (8), which is derived as

$$\sigma_{\mathrm{n}}{}^2=\frac{1}{N-L_{\mathrm{cp}}}\sum_{n=L_{\mathrm{cp}}}^{N-1}\left|\mathrm{IDFT}_N(\hat{\boldsymbol{H}}_{\mathrm{LS}})\right|^2 \tag{13}$$

where $\mathrm{IDFT}_N(\cdot)$ represents the inverse DFT operation of the N point.

Let $\boldsymbol{D}_{\mathrm{P}}=\boldsymbol{X}_{\mathrm{P}}$, take it into (11) to get the initial CIR estimate

$$\hat{\boldsymbol{h}}=\left(\boldsymbol{A}^{\mathrm{H}}\boldsymbol{A}\right)^{-1}\boldsymbol{A}^{\mathrm{H}}\boldsymbol{Y}_{\mathrm{P}}=\left[\left(\boldsymbol{X}_{\mathrm{P}}\boldsymbol{F}_{P\times L_{\mathrm{cp}}}\right)^{\mathrm{H}}\left(\boldsymbol{X}_{\mathrm{P}}\boldsymbol{F}_{P\times L_{\mathrm{cp}}}\right)\right]^{-1}\left(\boldsymbol{X}_{\mathrm{P}}\boldsymbol{F}_{P\times L_{\mathrm{cp}}}\right)^{\mathrm{H}}\boldsymbol{Y}_{\mathrm{P}}. \tag{14}$$

The decision rule for retaining the MST can be improved as

$$\hat{h}_{\mathrm{prop}}(l)=\begin{cases}\hat{h}(l), & \left|\hat{h}(l)\right|>T_{\mathrm{h}}\\ 0, & \left|\hat{h}(l)\right|\leqslant T_{\mathrm{h}}\end{cases} \tag{15}$$

where $0\leqslant l<L_{\mathrm{cp}}$.

(ii) Reduce the effect of strong nonlinear PA distortion by decision-aided operation.

Simulate the distorted pilot after the PA distorts the signal. The initial signal estimation can be obtained by making a hard decision based on the constellation

$$\hat{\boldsymbol{X}}=\mathrm{HardDecision}\left(\frac{\boldsymbol{Y}}{\boldsymbol{H}_{\mathrm{prop}}}\right) \tag{16}$$

where $\boldsymbol{H}_{\mathrm{prop}}\in\mathbf{C}^{N\times 1}$ is the complete frequency-domain CIR obtained by the proposed method, which is interpolated from the frequency-domain CIR $\boldsymbol{F}_{P\times L_{\mathrm{cp}}}\hat{\boldsymbol{h}}_{\mathrm{prop}}$ at the pilot. Perform PA distortion operation, then we have

$$\hat{\boldsymbol{d}}=g\left[\mathrm{IDFT}_N\left(\hat{\boldsymbol{X}}\right)\right]. \tag{17}$$

Perform a DFT operation on $\hat{\boldsymbol{d}}$ to obtain $\hat{\boldsymbol{D}}$, and then get the distorted pilots $\hat{\boldsymbol{D}}_{\mathrm{P}}$. The decision-aided (DA) operation is summarized in Algorithm 1.

Algorithm 1 DA algorithm

Input: $\boldsymbol{Y}$, $\boldsymbol{F}_{P\times L_{\mathrm{cp}}}$, $\hat{\boldsymbol{h}}_{\mathrm{prop}}$, $g[\cdot]$, I_{P}

Output: $\hat{\boldsymbol{D}}_{\mathrm{P}}$

Steps:

1: **Initial signal estimation**

$\hat{\boldsymbol{X}}=\mathrm{HardDecision}[\boldsymbol{Y}/\boldsymbol{H}_{\mathrm{prop}}]$.

2: **PA distortion** $\hat{\boldsymbol{d}} = g\left[\mathrm{IDFT}_N\left(\hat{\boldsymbol{X}}\right)\right]$.

3: **Distorted pilots** $\hat{\boldsymbol{D}}_{\mathrm{P}} = \left[\mathrm{DFT}_N\left(\hat{\boldsymbol{d}}\right)\right]_{I_{\mathrm{P}}}$.

(iii) Set $\boldsymbol{D}_{\mathrm{P}} = \hat{\boldsymbol{D}}_{\mathrm{P}}$, and repeat (i) to get the final channel estimation result $\hat{\boldsymbol{h}}_{\mathrm{prop}}$.

Reserving the MST is directly affected by threshold T_{h} determined by the channel noise vector $\boldsymbol{h}_{\mathrm{n}}$. Since the frequency-domain LS channel estimation performance in the uniform pilot pattern is better than that in other pilot patterns, the effective threshold is calculated based on LS results. At the same time, according to the signal detection results, the distorted pilot is obtained by simulating the transmitted signal through the PA distortion operation. To reduce the influence of nonlinear distortion, it is necessary to use distorted pilots for channel estimation.

3.2 Random pilot pattern

The existing pilot distribution research focuses on the random pilot design to improve the data transmission rate [27]. The random pilot pattern is shown in Fig. 4. The restricted isometry property (RIP) of the compressed sensing theory indicates that the measurement using a random matrix guarantees a high probability of sparse recovery, that is, the randomly generated pilot mode is statistically optimal. Uniform pilot distribution is optimal only for least squares channel estimation methods [19].

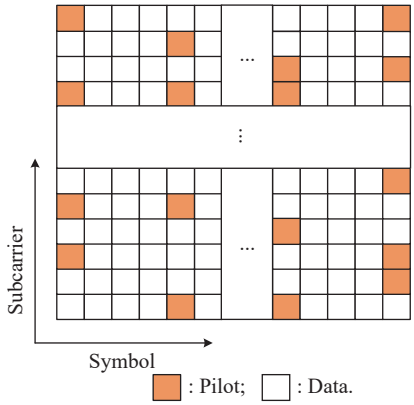

Fig. 4 Random pilot pattern

With $P < L_{\mathrm{cp}}$ and the random pilot pattern, we must explore the sparse characteristics of wireless multipath channels and use sparse recovery instead of the time-domain LS. Details of the proposed method are introduced.

(i) Sparse channel estimation is obtained based on adaptive sparsity.

The LS frequency-domain channel estimation and the effective channel threshold T_{h} are calculated by (8) and (12), respectively. The LS frequency-domain estimation result is compared with the threshold to obtain the time-domain channel sparsity $\hat{K}$ according to the following rules:

$$\hat{K} = \sum_{n=1}^{N} f\left[\mathrm{IDFT}_N(\hat{\boldsymbol{H}}_{\mathrm{LS}})\right] \tag{18}$$

where the function $f[\cdot]$ is defined as

$$f\left[\mathrm{IDFT}_N(\hat{\boldsymbol{H}}_{\mathrm{LS}})\right] = \begin{cases} 1, \left|\mathrm{IDFT}_N(\hat{\boldsymbol{H}}_{\mathrm{LS}})\right| > T_{\mathrm{h}} \\ 0, \left|\mathrm{IDFT}_N(\hat{\boldsymbol{H}}_{\mathrm{LS}})\right| \leqslant T_{\mathrm{h}} \end{cases}. \tag{19}$$

The detailed procedure for the orthogonal matching pursuit method with adaptive sparsity (AS-OMP) is summarized in Algorithm 2.

Algorithm 2 AS-OMP algorithm

Input: $\boldsymbol{Y}$, $\boldsymbol{A}$, $\hat{K}$

Output: $\hat{\boldsymbol{h}}_{\mathrm{prop}}$

Steps:

1: **Initialization**

- Residual vector $\boldsymbol{r}_0 = \boldsymbol{Y}$.
- Index set $\Lambda_0 = \varnothing$.
- Channel vector $\hat{\boldsymbol{h}} = \boldsymbol{0}^{L_{\mathrm{cp}} \times 1}$.

2: **For** $k = 1, 2, \cdots, \hat{K}$ **do**

Find the index $\Gamma_k = \arg \max_{j=1,2,\cdots,L_{\mathrm{cp}}} \left|\langle \boldsymbol{r}_{k-1}, \boldsymbol{a}_j \rangle\right|$.

Update the index set $\Lambda_k = \Lambda_{k-1} \cup \Gamma_k$.

Compute the path gain $\hat{\boldsymbol{\theta}}_k = \left(\boldsymbol{A}_{\Lambda_k}^{\mathrm{H}} \boldsymbol{A}_{\Lambda_k}\right)^{-1} \boldsymbol{A}_{\Lambda_k}^{\mathrm{H}} \boldsymbol{r}_{k-1}$.

Update the residual vector $\boldsymbol{r}_k = \boldsymbol{r}_{k-1} - \boldsymbol{A}_{\Lambda_k} \hat{\boldsymbol{\theta}}_k$.

End for

Reconstruct channel vector $\hat{\boldsymbol{h}}_{\Lambda_k} = \hat{\boldsymbol{\theta}}_k$.

3: **Output** $\hat{\boldsymbol{h}}_{\mathrm{prop}} = \hat{\boldsymbol{h}}$.

(ii) DA reduces the effect of strong nonlinear PA distortion. Refer to Algorithm 1 for details.

(iii) Set $\boldsymbol{D}_{\mathrm{P}} = \hat{\boldsymbol{D}}_{\mathrm{P}}$, and repeat (i) to get the final channel estimation result $\hat{\boldsymbol{h}}_{\mathrm{prop}}$.

For a given delay, sampling by a non-integer multiple and subsequent leakage effects increase channel sparsity. Due to the poor performance of LS in the frequency domain in random pilot patterns, the threshold calculated by (12) is not accurate enough. Therefore, the sparsity in our proposed AS-OMP algorithm depends on the relative value of the LS result compared with the threshold. Similar to the method proposed in the uniform pilot pattern, the distorted pilot is still obtained by using the DA algorithm, and the distorted pilot is used to further improve the channel estimation performance.

4. Simulation results

In this section, the normalized mean square error (NMSE) of the CIR is defined as

$$\mathrm{NMSE} = \frac{1}{G} \sum_{g=0}^{G-1} \frac{\left\|\hat{\boldsymbol{H}}_g - \boldsymbol{H}_g\right\|_2^2}{\left\|\boldsymbol{H}_g\right\|_2^2}, \tag{20}$$

where $\boldsymbol{H}_g$ and $\hat{\boldsymbol{H}}_g$ represent the real and the estimated channel state information (CSI) in the frequency domain, respectively. The NMSE and the BER are obtained by averaging over 100 independent Monte Carlo runs. The system is equipped with 512 subcarriers, 66.67 μs useful symbol duration, equal bandwidth sampling, 128 CP length, data, and pilot modulation of 16 quadrature amplitude modulation (16QAM) and 4QAM respectively. The average signal power is 1, the SEL model is used for the PA, and the passive radar coherent integration time is 0.25 s. The radar reference channel and communication channel are extended typical urban (ETU) models [28]. OFDM symbols with pilots appear every three OFDM symbols, of which 128 pilots are evenly distributed or 100 pilots are randomly distributed.

The system's overall performance is evaluated according to the NMSE, the BER, and the range-Doppler (RD) map of the target at different PA saturation amplitudes. The selection of saturation amplitude depends on the PA model. The passive radar detection is demonstrated in the scene where the reference channel's SNR is 40 dB, the surveillance channel's SNR is 35 dB, and other parameters are shown in Table 1.

Table 1 Surveillance channel parameters

Parameter	Multipath	Target
Delay/s	$[0, 0.1, 0.25, 0.38]\times10^{-6}$	$[15, 38, 58]/f_s$
Gain/dB	[−5.5, −7.8, −8.2, −11.9]	[−50, −60, −45]
Doppler/Hz	[0, 0, 0, 0]	[80, 160, −40]

In the data results, the LS frequency-domain method obtained by (7) without considering pilot distortion is called "traditional LS (standard pilots)". The result obtained by (8) with known distorted pilots is called "traditional LS (distorted pilots)". The operation of using the DA algorithm to reduce the nonlinear distortion for the channel result of [29] is called the "method in [29] + DA". In addition, we also refer to the methods in [12] and [20].

4.1 Performance in uniform pilot pattern

In Fig. 5 and Fig. 6, the NMSE and the BER performance of methods using the DA algorithm to assist channel estimation are better than those without considering pilot distortion. The traditional LS method has the worst channel estimation performance because it ignores the pilot distortion and the sparseness of the channel. Assuming the distorted pilots are known to the receiver, the performance of the LS is still limited because the MST is not preserved. The proposed method performs better than those methods in [12,29], thanks to the more efficient time domain channel thresholds.

According to the input and output characteristics of the PA, the lower the saturation level, the greater the distortion of the PA [8]. It can be seen from Fig. 5 that the NMSE performance gap of the proposed method before and after using the DA algorithm to compensate for pilot distortion increases as the saturation amplitude decreases. The trend of the NMSE performance gap between the standard pilot and the distorted pilot used by the LS method is similar to that of the proposed method.

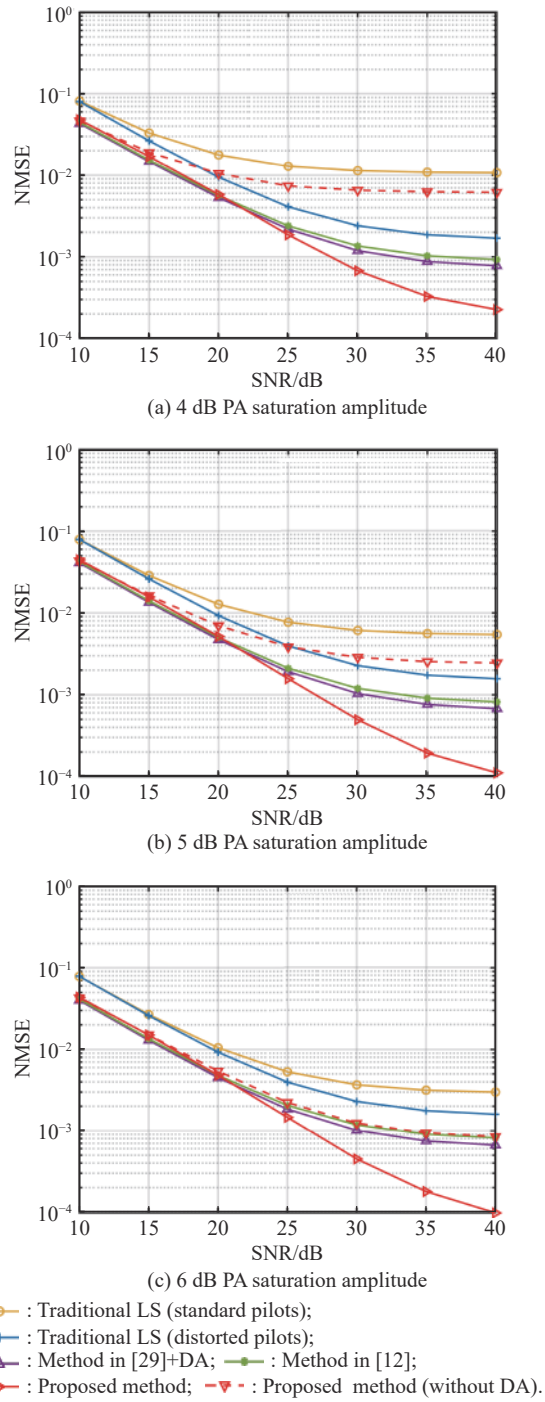

Fig. 5 NMSE performance of different channel estimation methods with the uniform pilot pattern

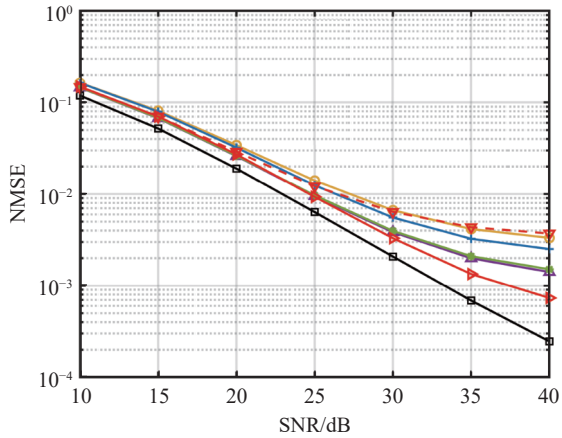

(a) 4 dB PA saturation amplitude

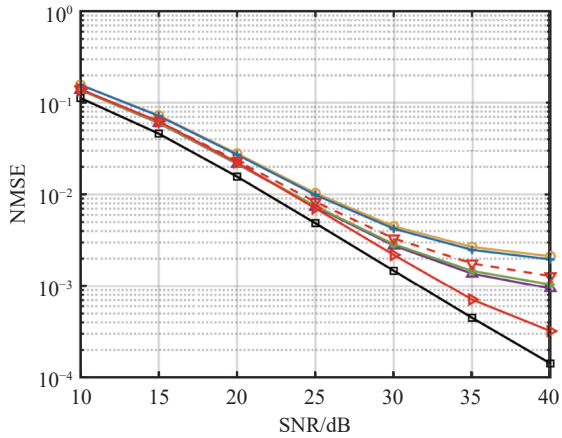

(b) 5 dB PA saturation amplitude

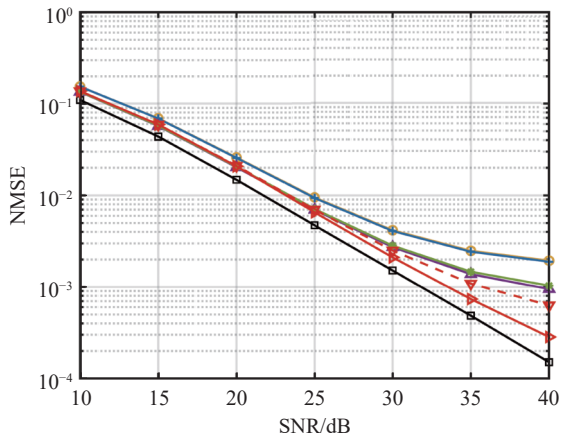

(c) 6 dB PA saturation amplitude

: Traditional LS (standard pilots);
: Traditional LS (distorted pilots);
: Method in [29]+DA; : Method in [12];
: Perfect CSI; : Proposed method;
: Proposed method (without DA).

Fig. 6 BER performance of different channel estimation methods with the uniform pilot pattern

According to the BER performance in Fig. 6, since the BER performance of the system is also related to the modulation constellation and the SNR, the channel estimation performance obtained by LS method (standard pilots) and LS method (distorted pilots) at low saturation amplitude is limited, resulting in the overall poor BER performance at 4 dB saturation amplitude. By analyzing the BER performance curve difference of the proposed method, the lower saturation amplitude leads to greater pilot signal distortion, increasing the error of the proposed method in acquiring sparse channels in the first step. Therefore, the BER performance gap before and after the proposed method uses the DA algorithm to compensate for pilot distortion also increases with the decrease of the PA saturation amplitude. Due to the strong nonlinear distortion results in greater channel noise, and this indicates that strong nonlinear distortion cannot be ignored in channel estimation.

The passive radar parameter settings are shown in Table 1. The reference signals reconstructed by different methods are used to suppress clutter in the surveillance channel under uniform pilot frequency. The RD map generated by two-dimensional matched filtering is shown in Fig. 7.

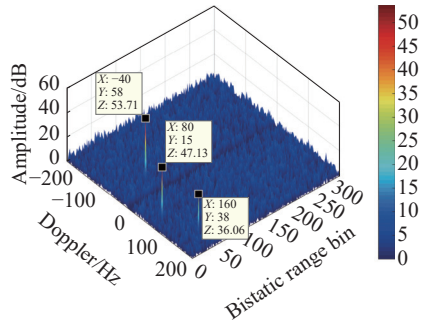

(a) Perfect CSI

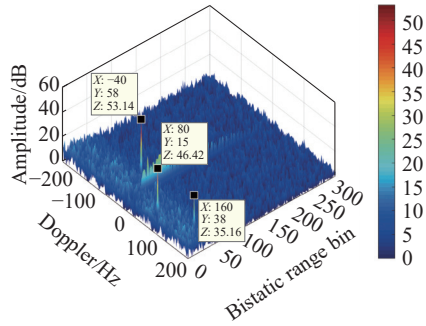

(b) Method in [12]

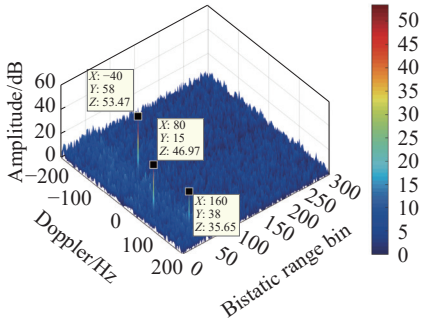

(c) Proposed method

Fig. 7 RD map of different channel estimation methods with the uniform pilot pattern (4 dB PA saturation amplitude)

Assuming that the perfect CSI is known, the ideal transmission signal can be obtained by reconstructing the reference signal, the clutter suppression processing effect is the best, and three targets with different strengths in the far and near can be displayed. Because the channel estimation accuracy of the method in [12] is not as good as that of the proposed method, the purity of the reconstructed reference signal is low, and the corresponding near range dimensional RD map has more clutter residues, which will affect the near range target detection with lower energy. Because the channel estimation performance of the proposed method is better than that of the method in [12], the clutter suppression effect is better, and the target detection performance on the RD spectrum is closer to the detection performance corresponding to the perfect CSI.

4.2 Performance in random pilot pattern

From Fig. 8 and Fig. 9, the LS methods and method in [12] have similar poor NMSE and BER performance. The empirical value set by the method in [20] is not universal as the stopping iteration condition of the OMP, resulting in its performance instability at low SNR and strong nonlinear distortion. The NMSE and BER performance of the proposed method is better than other methods. With the increase of distortion, the performance difference between the proposed method before and after using the DA algorithm is greater.

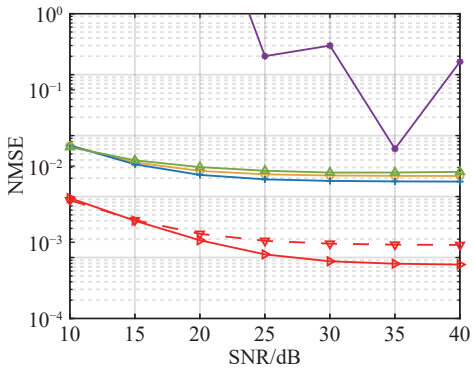

(a) 4 dB PA saturation amplitude

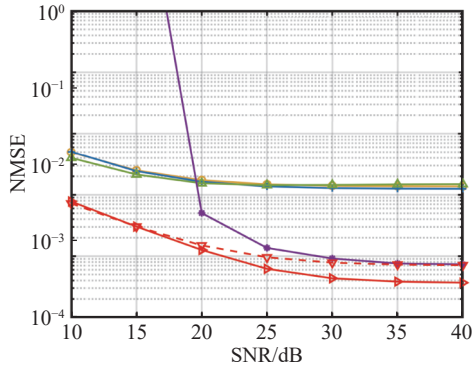

(b) 5 dB PA saturation amplitude

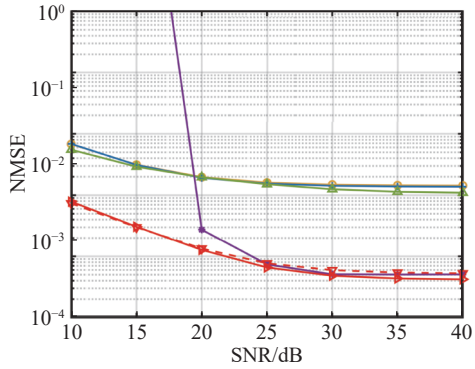

(c) 6 dB PA saturation amplitude

: Traditional LS (standard pilots);
: Traditional LS (distorted pilots);
: Method in [12]; : Method in [20];
: Proposed method ; : Proposed method (without DA).

Fig. 8 NMSE performance of different channel estimation methods with the random pilot pattern

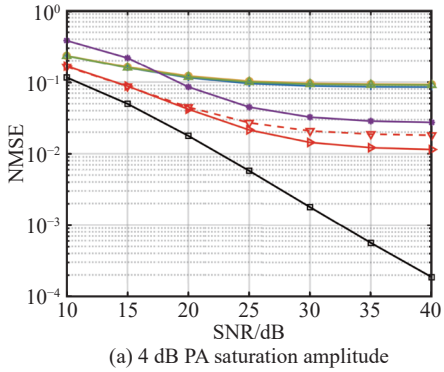

(a) 4 dB PA saturation amplitude

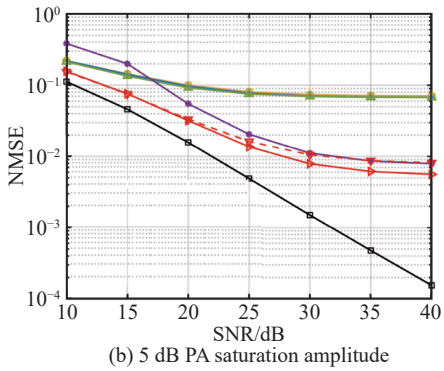

(b) 5 dB PA saturation amplitude

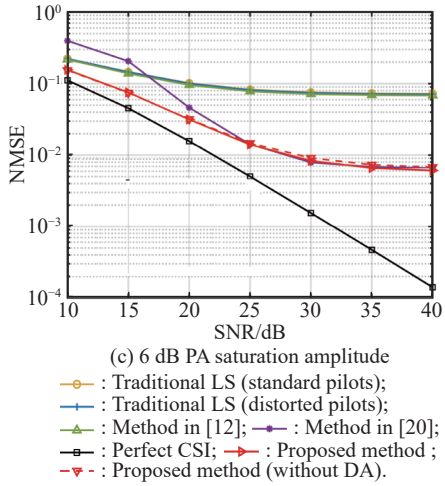

Fig. 9 BER performance of different channel estimation methods with the random pilot pattern

In Fig. 10, due to the reconstructed reference signal of the proposed method is closer to the transmitted signal, the clutter suppression effect is more obvious. The noise base in the RD map of the proposed method is lower and flatter than that of the method in [20], which makes it easier to distinguish targets. In Fig. 10 (b), the second target has the lowest SNR and cannot be identified from the noise base. Compared with Fig. 10 (a), the SNR loss of targets in Fig. 10 (b) is smaller than that of the method in [20], but it cannot be ignored. Because the random pilot under the simulation parameters is not optimized, its channel estimation performance is limited, resulting in a significant loss of targets' SNR. In addition, the pilot design and clutter suppression research can further improve the detection performance, but these are beyond our work [19,30].

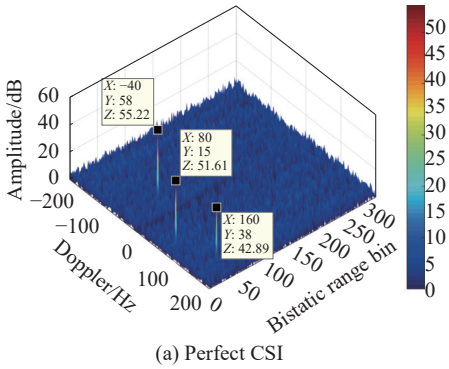

(a) Perfect CSI

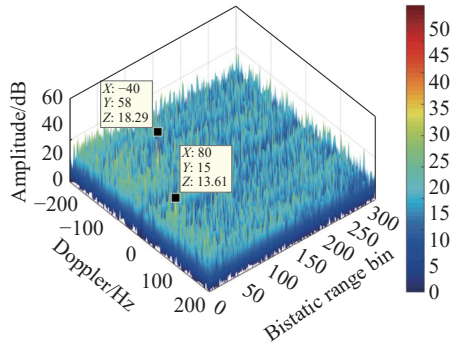

(b) Method in [20]

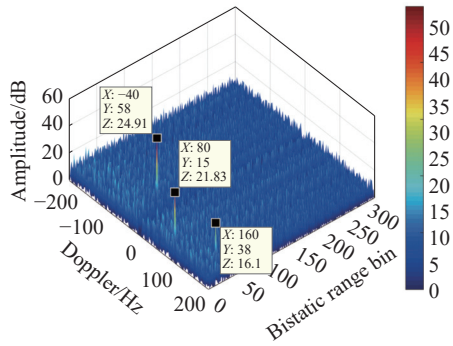

(c) Proposed method

Fig. 10 RD map of different channel estimation methods with the random pilot pattern (4 dB PA saturation amplitude)

5. Conclusions

In this paper, we propose channel estimation methods in nonlinear distortion scenarios to mitigate the impact of distortion on data transmission and target detection for the RadCom system. The key insight is to jointly use pilot distortion compensation and channel sparsity characteristics, and take different effective MST reservation operations according to different pilot patterns to improve channel estimation accuracy. Specifically, we use the LS frequency-domain channel estimation results to obtain the preliminary channel estimation results, and then reserve the channel coefficients that exceed the effective threshold to obtain the sparse channel results. Finally, we use the PA model to compensate for the distortion of the signal to obtain the distortion compensation channel results. The numerical results show that the proposed method has higher channel estimation accuracy and better comprehensive performance than the conventional method.

It is difficult but meaningful to quantitatively analyze the impact of the proposed scheme on radar detection performance under different PA distortion models. Therefore, our future work will focus on how to quantitatively analyze the impact of PA distortion on radar detection performance and design waveforms to reduce nonlinear distortion.

References

[1] OLIVEIRA L G D, NUSS B, ALABD M B, et al. Joint radar-communication systems: modulation schemes and system design. IEEE Trans. on Microwave Theory and Techniques, 2022, 70(3): 1521–1551.

[2] LIU Y J, LIAO G S, YANG Z W, et al. Design of integrated radar and communication system based on MIMO-OFDM waveform. Journal of Systems Engineering and Electronics, 2017, 28(4): 669–680.

[3] WU Q Q, XU J, ZENG Y, et al. Comprehensive overview on 5G-and-beyond networks with UAVs: from communications to sensing and intelligence. IEEE Journal on Selected Areas in Communications, 2021, 39(10): 2912–2945.

[4] ZHANG J A, RAHMAN M L, HUANG X J, et al. Enabling joint communication and radar sensing in mobile networks-a survey. IEEE Communications Surveys & Tutorials, 2022, 24(1): 306–345.

[5] LIU Y, YI J X, WAN X R, et al. PAPR reduction of OFDM waveform in integrated passive radar and communication systems. IEEE Sensors Journal, 2022, 22(17): 17307–17317.

[6] KUSCHEL H, CRISTALLINI D, OLSEN K E. Tutorial: passive radar tutorial. IEEE Aerospace and Electronic Systems Magazine, 2019, 34(2): 2–19.

[7] EVERS A, JACKSON J A. Cross-ambiguity characterization of communication waveform features for passive radar. IEEE Trans. on Aerospace and Electronic Systems, 2015, 51(4): 3440–3455.

[8] RAHMATALLAH Y, MOHAN S. Peak-to-average power ratio reduction in OFDM systems: a survey and taxonomy. IEEE Communications Surveys & Tutorials, 2013, 15(4): 1567–1592.

[9] BANELLI P, CACOPARDI S. Theoretical analysis and performance of OFDM signals in nonlinear AWGN channels. IEEE Trans. on Communications, 2000, 48(3): 430–441.

[10] ZHENG Z W. Effects of power amplifier distortion and channel estimation errors on the performance of DVB-H system with multiple-antenna receiver. IEEE Trans. on Consumer Electronics, 2009, 55(4): 1810–1818.

[11] GUERREIRO J, DINIS R, MONTEZUMA P. Optimum and sub-optimum receivers for OFDM signals with strong nonlinear distortion effects. IEEE Trans. on Communications, 2013, 61(9): 3830−3840.

[12] WU B Y, CHENG S X, CHEN M, et al. An adaptive channel estimation in clipped OFDM. Proc. of the IEEE International Symposium on Microwave, Antenna, Propagation and EMC Technologies for Wireless Communications, 2005: 1100−1103.

[13] MA X, KOBAYASHI H, SCHWARTZ S C, et al. Iterative channel estimation for OFDM with clipping. Proc. of the IEEE International Symposium on Wireless Personal Multimedia Communications, 2002: 1304−1308.

[14] OLFAT E, BENGTSSON M. Joint channel and clipping level estimation for OFDM in IoT-based networks. IEEE Trans. on Signal Processing, 2017, 65(18): 4902–4911.

[15] YE H, LI G Y, JUANG B H. Power of deep learning for channel estimation and signal detection in OFDM systems. IEEE Wireless Communications Letters, 2018, 7(1): 114–117.

[16] QING C J, DONG L, WANG L, et al. Joint model and data-driven receiver design for data-dependent superimposed training scheme with imperfect hardware. IEEE Trans. on Wireless Communications, 2022, 21(6): 3779–3791.

[17] ZHENG X, LAU V K N. Simultaneous learning and inferencing of DNN-based mmWave massive MIMO channel estimation in IoT systems with unknown nonlinear distortion. IEEE Internet of Things Journal, 2022, 9(1): 783–799.

[18] ZHANG X, YI J X, WAN X R, et al. Reference signal reconstruction under oversampling for DTMB-based passive radar. IEEE Access, 2020, 8: 74024–74038.

[19] QI C H, YUE G S, WU L N, et al. Pilot design schemes for sparse channel estimation in OFDM systems. IEEE Trans. on Vehicular Technology, 2015, 64(4): 1493–1505.

[20] WANG Z Z, LI Y Z, WANG C C, et al. A-OMP: an adaptive OMP algorithm for underwater acoustic OFDM channel estimation. IEEE Wireless Communications Letters, 2021, 10(8): 1761–1765.

[21] HOU S, WANG Y F, ZENG T Y, et al. Sparse channel estimation for spatial non-stationary massive MIMO channels. IEEE Communications Letters, 2020, 24(3): 681−684.

[22] LI T Y, LI D, YI X Y, et al. A sparse channel estimation scheme combined with distorted signal detection for UWB OFDM systems. IEEE Wireless Communications Letters, 2022, 11(7): 1438–1442.

[23] NAM H, KIM J, JEON J, et al. High-performance RF power amplifier module using optimum chip-level packaging structure. IEEE Trans. on Industrial Electronics, 2022, 69(6): 5660–5668.

[24] BALTI E, GUIZANI M. Impact of non-linear high-power amplifiers on cooperative relaying systems. IEEE Trans. on Communications, 2017, 65(10): 4163–4175.

[25] TELLADO J, HOO L M C, CIOFFI J M. Maximum-likelihood detection of nonlinearly distorted multicarrier symbols by iterative decoding. IEEE Trans. on Communications, 2003, 51(2): 218–228.

[26] BAJWA W U, HAUPT J, SAYEED A M, et al. Compressed channel sensing: a new approach to estimating sparse multipath channels. Proceedings of the IEEE, 2010, 98: 1058–1076.

[27] LI T Y, NOELS N, KAPUSUZ K Y, et al. Adaptive pilot allocation for estimating sparse uplink MU-MIMO-OFDM channels. IEEE Trans. on Communications, 2022, 21(10): 8230–8244.

[28] 3GPP. User equipment (UE) radio transmission and reception. https://www.etsi.org/deliver/etsi_ts/136100_136199/13-6101/10.03.00_60/ts_136101v100300p.pdf.

[29] KANG Y, KIM K, PARK H. Efficient DFT-based channel estimation for OFDM system on multipath channels. IET Communications, 2007, 1(2): 197–202.

[30] YI J X, WAN X R, LI D S, et al. Robust clutter rejection in passive radar via generalized subband cancellation. IEEE Trans. on Aerospace and Electronic Systems, 2018, 54(4): 1931–1946.

Biographies

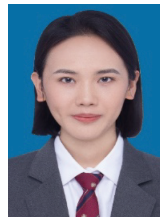

LIU Yan was born in 1993. She received her M.S. degree in electronic and communication engineering from Chongqing University of Posts and Telecommunications in 2018. She is currently pursuing her Ph.D. degree with the School of Electronic Information, Wuhan University. Her main research interests include the waveform design of dual-function radar and communication and its signal processing.

E-mail: liulynn@whu.edu.cn

YI Jianxin was born in 1989. He received his B.E. degree in electrical and electronic engineering, and his Ph.D. degree in radio physics from Wuhan University in 2011 and 2016, respectively. From August 2014 to August 2015, he was a visiting Ph.D. student at the University of Calgary. He is currently an associate professor with the School of Electronic Information, Wuhan University. His main research interests include radar signal processing, target tracking, and information fusion.
E-mail: jxyi@whu.edu.cn

WAN Xianrong was born in 1975. He received his B.E. degree in electrical and electronic engineering and Ph.D. degree in radio physics from Wuhan University in 1991 and 2005 respectively. He is currently a professor and a Ph.D. candidate supervisor with the School of Electronic Information, Wuhan University. His main research interests include design of new radar systems such as passive radars and over-the-horizon radars, and array signal processing.
E-mail: xrwan@whu.edu.cn

RAO Yunhua was born in 1972. He received his B.E. degree from Harbin Engineering University in 1995, and M.S. degree and Ph.D. degrees from Huazhong University of Science and Technology in 2000 and 2004, respectively. He is currently an associate professor with the School of Electronic Information, Wuhan University. His research interests include design of new radar system and wireless communication network.
E-mail: ryh@whu.edu.cn

HAO Caiyong was born in 1985. He received his B.S. and M.S. degrees from Hunan University in 2007 and 2010, respectively. He is currently pursuing his Ph.D. degree with the School of Electronic Information, Wuhan University, China. His research interests include radio spectrum monitoring, satellite communications, signal processing for wireless communications, and radio source localization.
E-mail: hao.c.y@srrc.org.cn